

Near 40-year drought trend during 1981-2019 earth warming and food security

Felix Kogan, Wei Guo & Wenzhe Yang

To cite this article: Felix Kogan, Wei Guo & Wenzhe Yang (2020) Near 40-year drought trend during 1981-2019 earth warming and food security, *Geomatics, Natural Hazards and Risk*, 11:1, 469-490, DOI: [10.1080/19475705.2020.1730452](https://doi.org/10.1080/19475705.2020.1730452)

To link to this article: <https://doi.org/10.1080/19475705.2020.1730452>



© 2020 The Author(s). Published by Informa UK Limited, trading as Taylor & Francis Group.



Published online: 26 Feb 2020.



Submit your article to this journal [↗](#)



Article views: 2979



View related articles [↗](#)




View Crossmark data [↗](#)



Citing articles: 9 View citing articles [↗](#)



Near 40-year drought trend during 1981-2019 earth warming and food security

Felix Kogan^a, Wei Guo^b and Wenze Yang^b 

^aCenter for Satellite Applications and Research, National Oceanic and Atmospheric Administration, National Environmental Satellite Data and Information Services, College Park, USA; ^bIMSG, College Park, USA

ABSTRACT

Following the 2014 report of the International Panel on Climate Change (IPCC), Earth surface has been warming up since the mid-18th century. From the late 1970s, Earth warmed up intensively, leading to unusual environmental, economic and social events. An intensive 19th century's, Earth warming has speeded up ice melting and sea level rise, increased water shortage and drought intensity. Expected drought intensification and expansion would reduce crop production, deteriorating food security and intensifying poor population's hunger. Since climate warming is continuing, we estimate long-term interaction between global warming and high-resolution drought tendencies and its consequences for global and regional food security. This paper develops and investigates satellite-derived 38-year high-resolution drought data sets and evaluate their trends, during 1981-2018. Drought was estimated using satellite-based Vegetation Health (VH) method. The results indicated that for the entire globe, hemispheres and the main grain-producing countries (China, USA and India) drought has not intensified and expanded during 38-year, while the global temperature anomaly has strongly increased. Since drought has not intensified and expanded during strong global warming, food security in the next few years is likely to remain at the level of the most recent decade.

ARTICLE HISTORY

Received 29 December 2019
Accepted 11 February 2020

KEYWORDS

Global warming; drought trend; NOAA-AVHRR data; Vegetation Health indices

Introduction

Since the mid-18th century, Earth climate has been warming up (IPCC 2007, 2014, 2018a, 2018b). From the 19th century, this process has intensified, especially since the late-1970s, when by the turn of the 20th century, global temperature anomaly (TA, relative to 1980-2010 climatology) increased up to 0.6 °C (IPCC 2014; NOAA 2017; WMO 2018b), leading to quite unusual environmental, economic and social events (IPCC 2014; NOAA 2016, 2017, NOAA/NCEI 2017; UNESCO 2018, NASA 2018b, 2017). Such a strong climate warming has been frequently reported to speed up ice

CONTACT Felix Kogan  Felix.Kogan@noaa.gov

© 2020 The Author(s). Published by Informa UK Limited, trading as Taylor & Francis Group.

This is an Open Access article distributed under the terms of the Creative Commons Attribution License (<http://creativecommons.org/licenses/by/4.0/>), which permits unrestricted use, distribution, and reproduction in any medium, provided the original work is properly cited.

melting in the northern pole and sea level rise, to affect changes in biological systems (plants, birds, insects etc.), to increase water scarcity and to deteriorate drought (Bromwich et al. 2013; IPCC 2014; Godfray et al. 2010; Chandler 2018; Coats 2018; FAO 2017, 2018; Serreze 2018; UNESCO 2018; Watts 2018; Eilpering et al. 2019). One of the most frequently cited (by climate publications and media) consequences of the recent 38-year global Earth warming for food security, was drought intensification and expansion, leading to a reduction of agricultural production, shortages of food and even hunger in developing countries of Africa, Southeast Asia and South America (NOAA 2016, 2017; WMO 2016, 2017, 2018b; FAO 2017, 2018; Charles et al. 2018; Najafi et al. 2018; Seager 2018). Experts from the United Nations are warning that continuation of climate warming, would further intensify and expand droughts leading to a stronger reduction of crop production, especially in developing countries, further deterioration of food security, leading to more intensive population malnutrition and hunger (FAO 2017; WMO 2017; UNESCO 2018).

Following continues climate warming and food security concerns (Coats 2018; Eilpering et al. 2019), a reasonable question to ask is what to expect in the near and distant future with anticipated drought intensification and expansion, water shortages and considerable increase in global and regional agricultural losses. These problems would deteriorate considerably food security, leading to more people suffering from hunger, especially considering that in the last 50-year, Earth population has been growing faster than the agricultural production (Brown 2012, 2013; Charles et al. 2018; Kogan 2018; Najafi et al. 2018; Kogan et al. 2019; Toulmin 2010). Many climate scientists predict that the Earth warming will affect not only developed but also developing countries. Since developing countries have been already suffering from a lack of food, drought intensification and expansion will increase agricultural losses deteriorating food security and well-being of nearly one-half of the world population. If droughts are more frequent, intensive and spreads to new areas, agricultural losses would be much larger, creating more problems with global and regional food supply. If agriculture would be less productive due to drought intensification and expansion, a negative difference between food supply and demand would be increasing much stronger and faster (IPCC 2014; WMO 2016; FAO 2017, 2018; Godfray et al. 2010; Kogan 2018; UNESCO 2018).

The recent 20-year climate-change scientific publications, covering drought dynamics and its impacts on the Earth environment, economy and food supply-demand, are based on less than two decades of wide-spread weather station data records for relatively local areas, rather than on analysis of multi-decadal global, hemispheric and the main agricultural countries' drought assessments (Bromwich et al. 2013; Christy 2017; ; FAO 2017; Forzieri et al. 2017; Godfray et al. 2010; Chandler 2018; IPCC 2014, 2018a, 2018b; Cheng et al. 2019). Therefore, the goals of this paper were to (a) analyze the 1981-2018 high-resolution (4 km², weekly) satellite-based, global and regional drought dynamics, (b) approximate changes in drought area and intensity, (c) estimate drought contribution to agricultural losses, (d) match the 1981-2018 global and regional drought dynamics with global TA trend and (e) investigate the consequences of drought changes during global warming for food security. This analysis is based

on high spatial and temporal resolution of global drought records, obtained from the National Oceanic and Atmospheric Administration (NOAA) operational afternoon polar-orbiting satellites. They were measuring weekly vegetation health (since 1981 for each 4 km² land surface) in response to moisture-thermal variations, including their extreme values, which cause vegetation stress, during the recent 38-year (Kogan 2018).

Vegetation Health

What is Vegetation Health?

The Vegetation Health (VH) is the state of vegetation in response to the environmental conditions. In general, if vegetation is intensively green (due to elevated chlorophyll contains), vigorous (due to substantial water content) and distributed uniformly over an area, it is considered to be healthy. In opposite situation, vegetation is yellow, wilting, not uniform (missing in some places) it is estimated to be stressed (Kogan 2018; Kogan et al. 2019). The quantitative measures of extreme and intermediate vegetation health are determined from satellite data. The 1981-2019 high-resolution weekly Vegetation Health data is derived from NOAA operational afternoon polar-orbiting satellite measuring reflected and emitted solar radiation from earth surface. During the 39-year of NOAA's satellites operation, two sensors were used the Advanced Very High Resolution Radiometer (AVHRR) from 1981 through 2012 and Visible Infrared Imaging Radiometer Suite (VIIRS) during 2013-2019. Both sensors were measuring reflected solar radiation in the visible (VIS) and near infrared (NIR) and emitted radiation in infrared (IR) wavelength (Kogan et al. 2015; Kogan 2018; Kogan et al. 2019). In VH development, NOAA data were thoroughly calibrated and processed to remove multiple sources of long- and short-term noise (technical, sensors' difference, environmental etc.), in order to receive reliable estimates of drought characteristics and trends. Almost four decades satellite data and derived indices were measuring global high-resolution pixel-based daily solar reflectance and emission. These original data were aggregated to 4.0 and 16 km² areal and one-week temporal resolution. Finally, the new satellite-based Vegetation Health methodology was applied to estimate vegetation performance, including drought-caused vegetation stress (Kogan and Guo 2014; Kogan 2018, 2001, 1997; Kogan et al. 2019). Important that VH-based drought was derived inside crops and pasture areas, rather than from air temperature and precipitation, measured at 2-m heights by a limited number of weather stations (principally used by climate research to estimate global and regional temperature trends (IPCC 2014, 2018a, 2018b; WMO 2018b; NOAA 2017; NASA 2017, 2018b)).

Original data

What is important for VH-based drought detection and estimation of its intensity and area coverage is that the VIS and NIR measurements characterize vegetation productivity following changes in photosynthetic rate (based on chlorophyll-a, -b and carotenoids content) and water content, while infrared (IR) measurements estimates

thermal conditions of vegetation cover. These moisture-thermal vegetation characteristics are regulated by climate and weather (Hashemi and Chenani 2004; Kogan 2018). Following physiological laws, several indices were developed, using VIS, NIR and IR measurements. Two initial indices included Normalized Difference Vegetation Index (NDVI) from VIS and NIR (Tucker 1979) and Brightness Temperature (BT) from IR (Trishchenko 2006) to characterize vegetation greenness and radiative (or brightness) temperature (equations 1 and 2, respectively).

$$\text{NDVI} = (\text{NIR} - \text{VIS})/(\text{NIR} + \text{VIS}) \quad (1)$$

$$\text{BT} = \left[\left(C_2 V_c / \log (C_1 V_c^3 / R + 1) \right) - B \right] / A \quad (2)$$

Where BT - brightness (radiation) temperature ($^{\circ}\text{K}$); R the observed IR ($\text{mWm}^{-2} \text{sr}^{-1} (\text{cm}^{-1})^{-1}$), $C_1 = 2hc^2$ and $C_2 = (hc)/k$, where c , h , and k are the speed of light, Planck-, and Boltzmann-constant, respectively; V - wavenumber (cm^{-1}); A, and B parameters are found from a non-linear regression of a pre-calculated lookup table.

Noise Removal is an extremely important procedure to be absolutely sure that drought time series, discussed below, are not distorted by long-term noise and are appropriate to identify correctly long-term trends. Therefore, before 38-year weekly drought time series were developed the original data and indices (NDVI and BT) have been intensively processed to remove noise. A short description below summarizes noise removal, which is comprehensively described in Kogan (2018). Daily VIS, NIR and BT values were calibrated comprehensively and the two initial indices (Equations 1 and 2) were calculated. Daily NDVI and BT data were aggregated to 7-day composite values for each 4.0 and 16.0 km^2 pixels of the global land (NOAA/NESDIS 2019). The sources of noise in NDVI and BT data are multiple. They include difference between the sensors (S-NPP/VIIRS from NOAA-20/VIIRS and VIIRS from AVHRR) and even between AVHRR-2 and AVHRR-3 sensors (due to difference in sensor design and response functions). Since the time of NOAA-7 through NOAA-18 satellite observation is changing from 1:30 pm at their launch to almost 6 pm at the end of satellite life due to orbital drift, this noise was carefully corrected. Long-term aerosol noise from El Chichon in 1982 and Mt. Pinatubo in 1991 (Kogan 2018, WMO 2017, NOAA 2016(IPCC 2018a)) volcanos was corrected using the Empirical Distribution Function (EDF). Besides long-term, short-term corrections have been performed, eliminating noise related to daily clouds and aerosols, sun-surface sensor geometry, bi-directional reflectance, open canopy background, difference in ecosystems, human errors and others. All of these corrections were accomplished and have been described in Kogan (2018). that the users were absolutely sure that the data are reliable to be used for drought trend analysis.

Vegetation Health indices

As the result of high- and low-frequency noise removal, NDVI and BT weekly time series were transferred to no-noise Smoothed NDVI (SMN) and Smoothed BT (SMT)

values (Kogan 2018). The SMN and SMT indices characterize two environmental components: the long-term ecosystem-climate (for example, tropical forest versus broad-leaf forest or grassland) and short-term, weather changes (daily-weekly-monthly (up to one year) precipitation, temperature etc.). Since the VH is designed for monitoring weather impacts (including drought) on vegetation, the long-term climate component was removed from SMN and SMT weekly data for each 4.0 km² pixel. Following three bio-physical laws: Liebig's Law-of-minimum, Sheffield's Law-of-tolerance and the Principle of Carrying Capacity, weather component was singled out for each week and pixel by normalizing SMN and SMT to the extreme 34-year (1981-2014), maximum (MAX) and minimum (MIN) weekly-pixel values of SMN and SMT, characterizing extremely favorable and unfavorable vegetation conditions or very healthy and unhealthy (or stressed) vegetation. Finally, three indices assessing weather-impact on vegetation were developed (Equations 3–5): Vegetation Condition Index (VCI), Temperature Condition Index (TCI) and Vegetation Health Index (VHI). VCI, TCI and VHI indices characterize vegetation health, specifically, moisture (VCI), thermal (TCI) and combined moisture-thermal (VHI) conditions.

$$VCI = 100 * (SMN - SMN_{min}) / (SMN_{max} - SMN_{min}) \quad (3)$$

$$TCI = 100 * (SMT_{max} - SMT) / (SMT_{max} - SMT_{min}) \quad (4)$$

$$VHI = a * VCI + (1-a) * TCI \quad (5)$$

Equation (5) contains coefficient a , which is used to estimate a portion of moisture and thermal conditions in the VHI's combine estimation of moisture-thermal based vegetation health. This share depends on VHI's application, ecosystem, climate, weather, season and others. Since, the share is generally not known for specific applications, it was assumed that VCI and TCI contributions are equal ($a = 0.5$). Meanwhile, a can be calibrated against ground measurements, such as biomass value, agricultural production, number of affected people by a disaster and others. Some examples of using calibrated a against crop yields in USA, China, Bulgaria and other countries are presented in Kogan (1983, 2001), Kogan et al. (2005), and Najafi et al. (2018). For a calibration we first, correlated 15-30 years' yield anomaly (for a region) with weekly VCI and TCI over the season (for example, March-September in the Northern Hemisphere). Second, used correlation coefficients values to derive their share.

The VCI, TCI and VHI indices estimate weather-related moisture (VCI), thermal (TCI) and combined moisture-thermal (VHI) conditions inside vegetation on a scale from zero, indicating extremely unhealthy or stress vegetation, to 100 specifying the healthiest vegetation. The VH indices (VCI, TCI and VHI) have been calibrated and validated based on crops and pasture yield anomaly in 34 countries, including principal producers of grain (Kogan 2018). The VH indices assess physiologically-based vegetation performance, on a scale from healthy to unhealthy, which are changing following weather fluctuation from favorable (warm and moist) to unfavorable (hot and dry), respectively. Vegetation Health indices are assigned values from zero (0) when vegetation is extremely stressed to 100 if vegetation is very healthy. In principal,

green, vigorous and uniformly distributed vegetation indicates that favorable weather (warm and wet) induced healthy conditions, estimated by high values of VH indices (56-100). In opposite case, not green (yellow-brown), wilting, not uniformly distributed vegetation indicates unfavorable weather conditions (dry and hot) inducing, vegetation stress (VH indices are below 46). These two opposite cases, healthy and unhealthy (or stressed) vegetation characterize two opposite vegetation conditions with several levels of intermedium vegetation performance for these two levels of vegetation condition values (healthy and unhealthy). The two extreme values (0 and 100) have generally low frequency over time and space.

Drought from Vegetation Health

Comparison of VH indices (VCI, TCI and VHI) with crop yields in 34 countries on all continents (Kogan 2018) indicated that drought and crop yield reduction usually start when the indices fluctuate between zero and 45 (Kogan 2018). Classification of drought intensity was based on the amount of corn yield reduction in the USA's corn-belt and reduction of spring wheat yield in the main area of Russia (Kogan 2018). Numerical drought estimates included several categories: light (indices between 45 and 36), moderate (35-26), severe (25-16), extreme (15-6) and exceptional (<6). Following this classification, VH is widely used for analysis of such drought features as start, intensity, area, duration, frequency and impact. The VH indices are normally applied to estimate vegetation stress from moisture, thermal and more frequently from combine moisture-thermal conditions. Drought might affect vegetation strongly from either moisture deficit or excessive heat or from their combine moisture-thermal stress (moisture deficit and excessive heat, which is the best estimates). Environmentally-based drought impacts on vegetation depend on severity and duration of combined moisture and thermal stress. Relatively mild stress (both moisture and thermal) produces minor impacts on vegetation in general, especially on crops and pasture. Severe stress produces major impacts, reducing crops and pasture production more than 50% (relative to multi-year mean values). Drought degrades natural vegetation as well. However, if only one of the parameters (moisture or thermal) is in extreme conditions drought impacts might be offset by favorable conditions from another parameter. For example, in case of extreme environmental heat, crops and pasture can survive for some time if there is no moisture deficit. In opposite case, if vegetation experience strong moisture deficit, its condition might deteriorate slowly if the weather is relatively cool. There are many such examples in scientific publications (Myneni et al. 1997; Lucht et al. 2002; Nemani et al. 2003; Murph and Timbal 2008; Godfray et al. 2010; Kogan 2018; Kogan et al. 2018). Meanwhile, if both moisture and thermal conditions are unfavorable or stressful, drought impacts on vegetation are estimated more accurately. Therefore, further discussion presents analysis of 38-year drought trends from the Vegetation Health Index (VHI), which provides combine moisture-thermal drought conditions during the entire period of intensive Earth warming. Specifically, VHI-based drought time-series were used for statistical trend assessments of different drought levels, and analysis if these trends are matching with intensive global warming trends. This is an important goal for

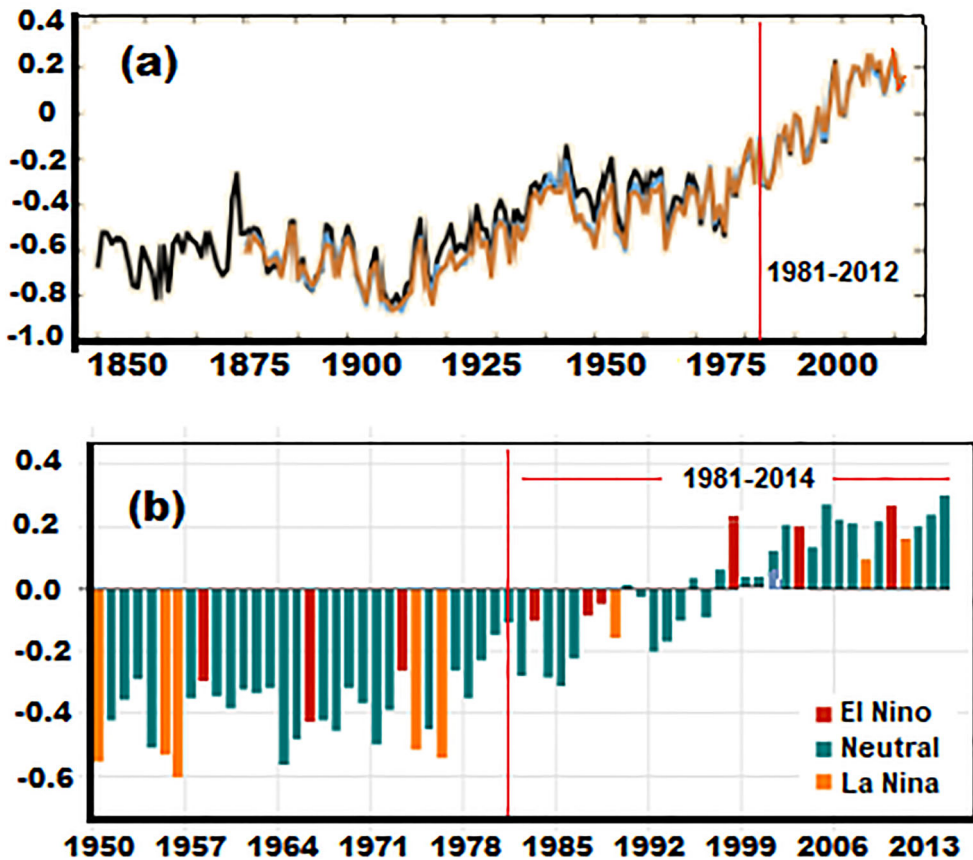


Figure 1. Annual global mean Earth temperature anomaly during (a) 1850–2012 (relative to 1886–2005 global mean annual temperature (from IPCC 2014, color indicates different data sets)) and (b) 1950–2014 (relative to 1981–2010 global mean annual temperature with an indication of ENSO years (WMO 2014)); red vertical lines indicate the period from 1981, when Vegetation Health data has started. Source: Author

estimation of the future tendencies in drought, vegetation stress and problems expected with agricultural production and food security.

Global warming

Following IPCC (2014, 2007, 2018a, 2018b) and other reports (Hansen et al. 2000, 2010; Karl et al. 2015; NOAA 2017; WMO 2014, 2017; NASA 2017, 2018b; UNESCO 2018), continuous general global warming has been going on since the mid-1850's (Figure 1a). However, the strongest global temperature increase occurred after the mid-1970s (better seen in Figure 1b). As IPCC (2014) indicates, "... the period from 1983 to 2012 was likely the warmest 30-year period of the last 1,400 years in the Northern Hemisphere...", when "... the global average combined land and ocean temperature data calculated as linear trend, show a warming of 0.85°C (0.65 to 1.06°C) during 1980–2012." Many other publications are also focusing on an intensive global warming since mid-1970s (NASA 2017; NOAA 2017; FAO 2018; IPCC

2018a, 2018b). The period of the intensive global warming practically coincides with availability of moisture-thermal VHI data set (started in 1981), which characterize physiological vegetation response to weather and climate (NOAA/NESDIS 2019). Therefore, further analysis is focusing on global warming and VHI-estimated drought trends since 1981. Figure 1b is showing global annual temperature anomaly presented by the World Meteorological Organization, following IPCC and other reports (IPCC 2014; Karl et al. 2015; NASA 2017; NOAA 2017; USGCRP 2017). The period from 1981 through 2014 is focusing on global annual temperature anomaly and its tendency during VHI data availability.

Analysis of global mean Earth temperature anomaly (TA) since 1981 in Figure 1b clearly indicates two periods with different TA trend: (1) strong TA growth (upward trend) during 17-year from 1981 through 1997, when TA increased from approximately -0.32 to $+0.20$ °C and (2) flat trend in TA (around $+0.2$ °C) during 17 years, between 1998 and 2014. Climatologists called the second 17-year period with flat TA trend “hiatus” time (Kennel 2014; Karl et al. 2015). It is interesting, that short-term trends in TA for both Hemispheres (Hansen et al. 2010) are similar to the described global two 17-year trends from 1981 in Figure 1, although Northern Hemisphere’s TA is showing more closed match with the globe. Following the two 17-year TA data (Figure 1b), it should be emphasized again strong increase in TA from 1981 through 1997 and flat trend during hiatus time from 1998 through 2014. Discussing drought trends, climate publications have indicated an intensification of global droughts due to higher evaporative demands in warmer climate and even development of mega droughts during 1981-1997 (IPCC 2014; Chandler 2018; FAO 2017, 2018; UNESCO 2018). They are also indicating strong drought activities during hiatus time (between 1998 and 2014) due to positive global TA around $+0.2$ °C (Karl et al. 2015; WMO 2016; NOAA 2017; USGCRP 2017; Thomas et al. 2018; Wendel 2018). Therefore, further analysis present (a) VHI-based drought trends during the indicated two 17-year periods (1981-1997 and 1998-2014), (b) comparison of drought trend with global TA trend during the same two periods and (c) investigation if drought and global TA trends have similar features and how close their trends are.

Drought dynamics during global warming from 1981 through 2014

World. Since climate publications (NOAA 2016, 2017; BAMS 2018; Chandler 2018; FAO 2017, 2018; Serreze 2018; UNESCO 2018; Watts 2018; 2016, 2018b) have strongly emphasized drought expansion and intensification during global warming from the end of 1970s, the VHI-based drought trend was investigated first for the two indicated periods of global warming (1981-1997 and 1998-2014) clearly seen in Figure 1b (WMO 2014). The TA time series from WMO (2014) were selected since the anomaly is derived relative to the most recent 30-year global temperature climatology (1980-2010). Three the most damaging to food security drought intensities were analyzed: severe-to-exceptional (S-to-E), which reduce grain production from 10 to 25%, extreme-to-exceptional (E-to-E), 26-35% grain reduction, and exceptional (E), more than 35% reduction (Kogan 2018). Trends in drought areas for these three

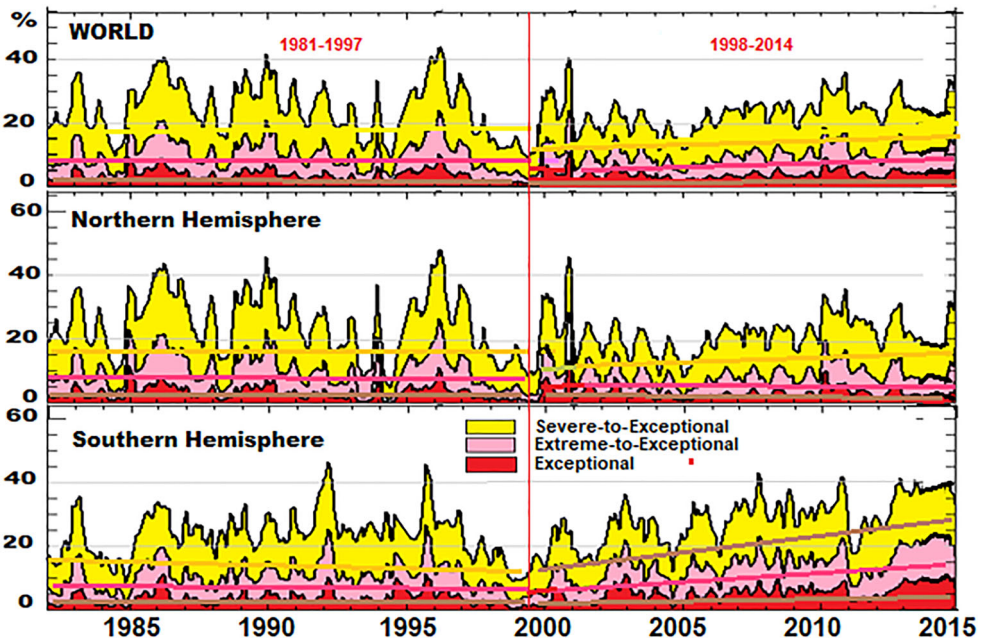


Figure 2. Drought area (% from the total world and hemispheres areas) and intensity (Severe-to-Exceptional, Extreme-to-Exceptional and Exceptional) for the World, Northern and Southern Hemispheres. Trend was statistically estimated for two 17-year periods, 1981-1997 and 1998-2014 (95% confidence level). Source: Author

intensities were estimated from satellite-based combined moisture-thermal condition index (VHI) during the two identified periods, 1981-1997 and 1998-2014.

Mean global and hemispheric multi-year weekly VHI-based drought time series and trends are shown in [Figure 2](#). They indicate that during 1981-2014, global drought has not intensified and has not expanded following strong global mean TA increase as was indicated by many climate publications (NOAA 2016, 2017; Chandler 2018; FAO 2017, 2018; NASA 2017, 2018b; Serreze 2018; UNESCO 2018; Watts 2018; 2016, 2018b). In spite of intensive global warming, the 1981-1997 global drought trends were stably flat (no increase and no decrease) for all intensities (18% for S-to-E, 8% for E-to-E and 4% for E), compare to a very strong global TA increase (from -0.32 to $+0.20$ °C). Oppositely, during the next 17-year (1998-2014), upward drought area and intensity trends (20-30% increase by 2014) appeared, while global TA had quite stable (flat) trend (TA nearly 0.2 °C) during the entire 1998-2014 period. Northern Hemisphere's drought trends for the three intensities were quite similar to the VHI-based world's drought tendencies. In Southern Hemisphere droughts occurred frequently during the two periods. However, opposite to the world and Northern Hemisphere, the Southern Hemisphere drought intensified and area increased from 1998 through 2014 almost 80-95%, mismatching with global TA flat trend. Summarizing, it should be emphasized again, that global and hemispheric VHI-derived two 17-year (1981-1997 and 1998-2014) drought trends mismatched with global TA trend. The world and both hemispheres' drought area and intensity (in all categories) have not changed, although the world warmed up considerably

Table 1. Grain production (million metric tons (MMT)), area (million hectares (MH), WB 2017) and (%) of their contribution to the world total.

| Continents and World | Country | Grain Production in 2014 | | Grain Area in 2014 | |
|----------------------|----------------|--------------------------|------------------|--------------------|------------------|
| | | Amount (MMT) | % from the World | Amount (MH) | % from the World |
| N. America | US | 442.8 | 15.7 | 58.4 | 8.1 |
| | Canada | 51.3 | 1.8 | 14.1 | 2.0 |
| | Mexico | 36.5 | 1.3 | 10.3 | 1.4 |
| Europe | France | 73.3 | 2.5 | 9.6 | 1.3 |
| | Germany | 52.0 | 1.8 | 6.3 | 0.9 |
| | Ukraine | 63.4 | 2.2 | 14.0 | 2.0 |
| Asia | China | 557.4 | 19.8 | 96.4 | 13.4 |
| | India | 296.4 | 10.5 | 98.5 | 13.7 |
| | Russia | 103.1 | 3.7 | 44.4 | 6.2 |
| | Indonesia | 89.8 | 3.2 | 18.1 | 2.8 |
| S. America | Brazil | 101.4 | 3.6 | 20.1 | 2.8 |
| | Argentina | 51.0 | 1.8 | 13.2 | 1.8 |
| Africa | Rep. S. Africa | 16.6 | 0.6 | 2.7 | 0.4 |
| | Ethiopia | 23.6 | 0.8 | 10.2 | 1.4 |
| Australia | Australia | 38.4 | 1.3 | 17.0 | 2.4 |
| WORLD | | 2,818.5 | 100.0 | 718.1 | 100.0 |

(slightly more than 0.5 °C) between 1981 and 1997. However, during a stable global TA from 1998 through 2014 (hiatus time) world drought area slightly increased (2-5%) for all intensities. However, in Southern Hemisphere, drought area and intensity trends have surprisingly increased strongly for S-to-E (100%) and E-to-E (80%) and moderately for E (30%), mismatching again with global flat trends, around +0.20 °C.

Principal grain countries

In addition to matching/mismatching the entire earth warming trend and global vegetation drought trend, similar drought analysis was performed in a few countries. Since drought have strong impacts on food security, this part investigates if strong global warming intensified droughts in the main grain producing countries and might result in a considerable reduction of agricultural production, creating problems with food security. These countries were selected based on their major contribution to the global grain production (the principal world's food and feed) in 2014 (WB 2017). Table 1 shows the main grain producers on each continent, their contribution to the world total grain production and occupied grain area. The three countries, which produced more than 10% of global grain in 2014, were selected for drought trend analysis. They were China (19.8% grain production contribution to the world total), USA (15.7% contribution) and India (10.5%). These three countries have produced almost 50% of global grain (the main agricultural production affecting strongly food security) in 2014 (Table 1). It is interesting that area-wise (Table 1), China (number one grain producer) and India (number 3) had practically the same grain area (98.5 and 96.4 million hectares (MH)), while the USA, being the second contributor to the global grain production, collected grain from 60% smaller area (58.4MH), which emphasizes an advancement in US agricultural technology.

Similar to global analysis, two 17-year (1981-1997 and 1998-2014) trends in drought area and intensities were investigate in China, USA and India. Figure 3

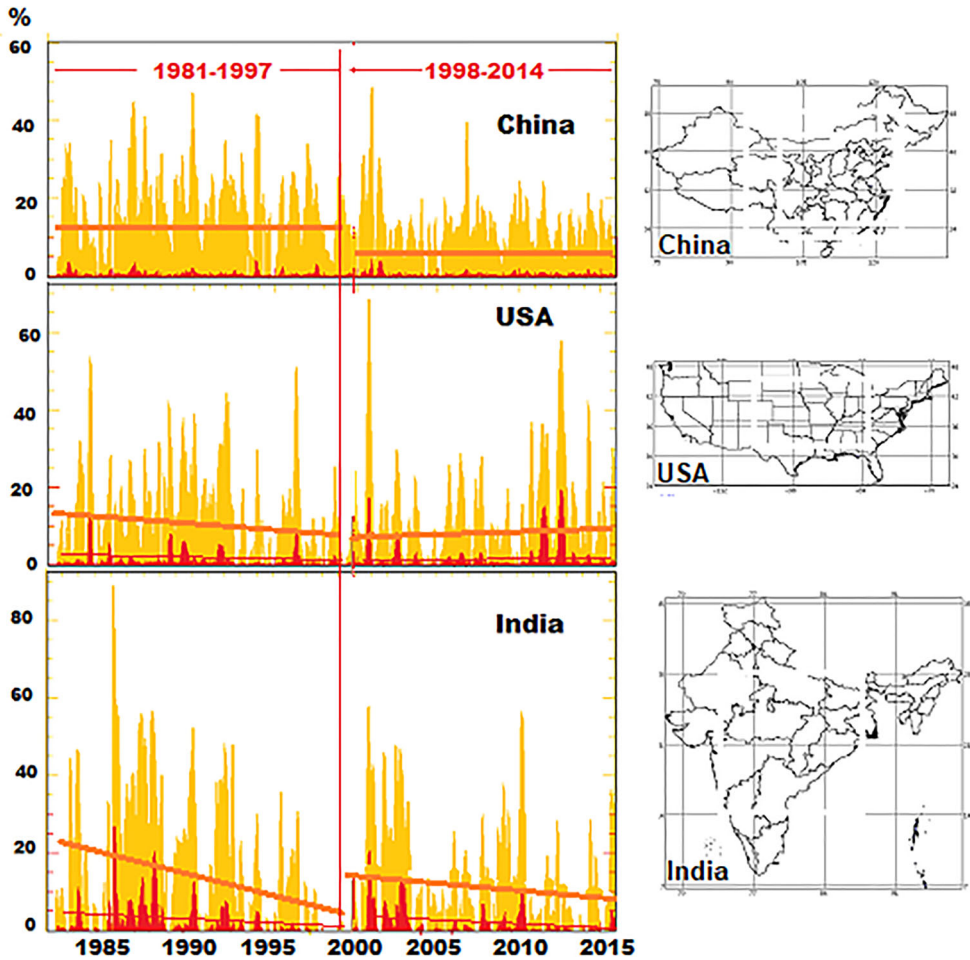


Figure 3. Weekly dynamics of drought area (percentage from a country) for two intensities (severe-to-exceptional (S-to-E), and exceptional (E) in China, USA and India. Trend was statistically estimated for the two 17-year periods, 1981-1997 and 1998-2014 with 95% confidence level. Source: Author

displays weekly drought area's time series and trends for the two intensities, severe-to-exceptional (S-to-E) and exceptional (E), which are frequent and the most damaging in these countries. Drought dynamics for the three countries (Figure 3) mismatched again (in some cases strongly) with global TA trends for both periods (Figure 1b). Specifically, in China (contributed 19.8% of global grain in 2014), drought area and intensity (in both categories) have not changed, occupying 14% and 1-2% of the country with S-to-E and E intensity, respectively, while the world warmed up strongly (mean global TA increased 0.52°C relative to 1980-2010 climatology) between 1981 and 1997. During the second 17-year, when the globe was stably warm at $+0.2^{\circ}\text{C}$ TA (Figure 1b), China's drought area reduced (surprisingly) in half, between 1998 and 2014, to 7% of the country for S-to-E intensity and remained stable at 1-2% of the country for E intensity. Drought tendencies in the USA and India performed differently than in China. During intensive global warming (1981-1997), drought area reduced slightly in the USA (from 13 to 9% for S-to-E and remained

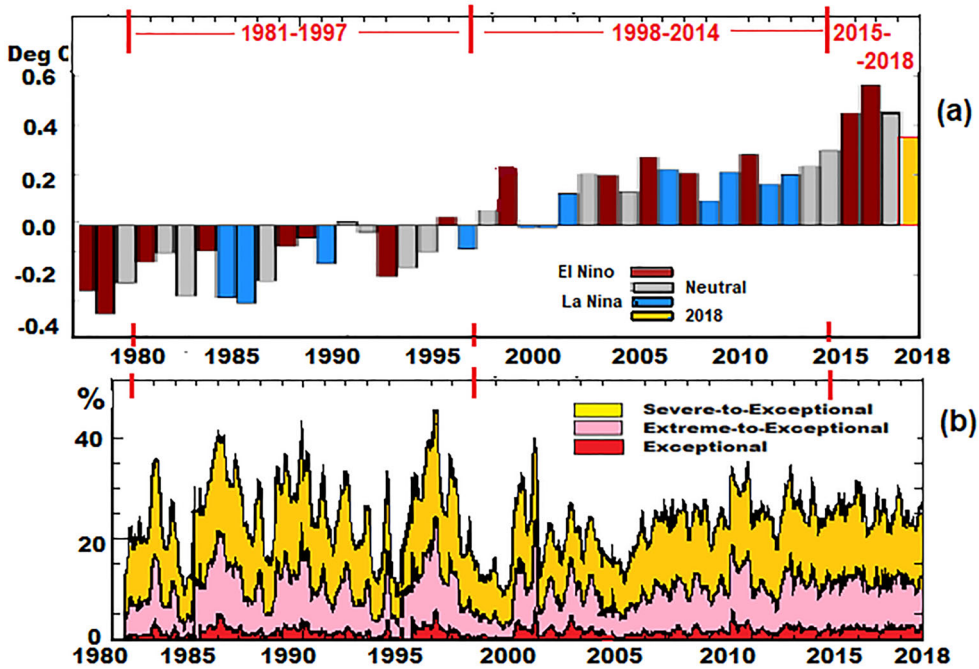


Figure 4. Global mean (a) Annual weekly temperature anomaly during 1950-2017 (relative to 1981-2010 mean annual temperature with emphasis on ENSO years (WMO 2018b)) and 2018 TA (relative to 1981-2010) from Spencer (2019); (b) Weekly VHI-based drought area and intensity (severe-to-exceptional (S-to-E), extreme-to-exceptional (E-to-E) and exceptional (E) with 95% confidence level) during 1981-2018. Source: Author

stable at 2-3% for E intensity) although global TA increased more than 0.5°C . In India, S-to-E intensity drought area surprisingly dropped three-time (from 23 to 7%), instead of expected increase following Earth warming (Figure 1b); an exceptional drought has slightly decreased as well. During the period of a stably warm globe between 1998 and 2014, the US drought area slightly increased (from 9 to 12% for S-to-E and remained stable, at 1-2% for exceptional intensity). Oppositely, to the USA, India's drought decreased nearly 30% (from 18 to 13%) for S-to-E and slightly decreased for E intensity. Summarizing, we should stress again that opposite to expected drought intensification and expansion due to global warming from 1981 through 2014 (2018b; NOAA 2016, 2017; Watts 2018; Serreze 2018; Kogan et al. 2013), the three major grain producing countries (China, USA and India) showed a reduced drought area trend for S-to-E and relatively stable drought trends for E intensity.

2015-2018 strong global warming and drought tendency

During 2015-2018, Earth temperature unexpectedly increased strongly. Figure 4a displays global temperature anomaly since 1980, shown in Figure 1b, but extended for the years 2015 through 2017 from WMO (2018a) and for 2018 from Spencer (2019). Calculations showed that four-year (2015-2018) mean global TA unexpectedly

reached 0.42°C , which was 0.22°C above the 17-year (1998-2014) flat global mean TA trend ($+0.2^{\circ}\text{C}$, relative to 1980-2010 climatology) during hiatus time. Detail analysis of these 4-year data (Figure 4a), indicate that in 2015, global mean TA (estimated relative to 1981-2010 global mean temperature climatology) jumped up to 0.45°C (from 0.2°C in 2014), in 2016, it increased even higher, to 0.56°C , and after that dropped down to 0.46°C in 2017 (WMO 2018a) and further down to 0.23°C in 2018 (Spencer 2019), quickly approaching to 1998-2014, hiatus time's TA trend level.

Climate publications indicated several causes for global mean TA increase, which are investigated including the latest 4-year. First of all, it is greenhouse gas emissions (mainly CO_2), since most of climate publications are strongly supporting contribution of industrial CO_2 release as the main cause of trapping earth-emitted infrared radiation, resulting in strong increase of Earth warming over the recent 3-4 decades (WMO 2018b, Blander et al. 2018; Williams & Roussenov 2017; NASA 2017; USGCRP 2017; IPCC 2014). However, CO_2 measurements (NASA 2018b) indicated that between 2014 and 2015, CO_2 has increased only 1% (from 397 to 400 Dobson Units), while global TA has more than doubled from 0.22 to 0.46°C , relative to 1980-2010 climatology (WMO 2018a) between these two years. Therefore, CO_2 contribution to doubling global mean TA between 2014 and 2015 (including the remaining three years) cannot be considered as one of the causes of strong 2015-2018 TA increase.

Another source of strong global TA increase in 2015 and especially 2016 (compared to 2014) was El Niño-Southern Oscillation (ENSO (USGCRP 2017; Blander et al. 2018; WMO 2018b)). During November 2015-April 2016, extreme El Niño occurred, when 3.4 ocean region in Tropical Pacific (the main ENSO area) was 3.0°C warmer than normal (Kogan and Guo 2017), which was the strongest ENSO in the past several decades. Release of such extreme ocean heat intensified overall global warming (Wendel 2018). A very warm 2015-16 El Niño contribution to global warming was also intensified by two other preceding events of a warm ocean: (a) the so-called "Blob" and (b) long-term accumulated ocean heat (Thomas et al. 2018; Cheng et al. 2019; Cornwall 2019). The Blob started in late 2013 (Cornwall 2019), when a large area of unusually warm water formed in a Gulf of Alaska has spread south so fast that by mid-2015, the Blob doubled in size, covered nearly $4 \times 10^6 \text{ km}^2$ of Pacific Ocean between Alaska and California, had surface temperature 2.5°C above normal and even crashed some of the marine ecosystems (appearance of toxic algae, small fish dying etc.) (Cornwall 2019). Regarding the (b) event, global ocean has been generally warming up for a few decades (Cheng et al. 2019). The rate of the warming for the upper 2000-m has accelerated from 0.55 in 1991 to 0.68 W m^{-2} by 2000. In addition, the area of warm ocean has increased strongly between 1982 and 2016 (from 27 to 62% for severe and from 68 to 93% for moderate heat (Cornwall 2019)). Moreover, the number of marine heat waves almost doubled during these years (Thomas et al. 2018). Therefore, release of heat accumulated in the ocean over the recent decades, heat from Blob during 2013-2015 and especially 2015-16 El Niño-released heat have contributed to the recent 4-year of Earth warming and can be considered as temporary events.

One more source of global warming during 2015-2018 was an unexpected and persistent increase in global emission of ozone-depleting chlorofluorocarbon (CFC),

specifically CFC-11 (Blander et al. 2018). The recent measurements indicated that CFC-11 was emitted from Southeast Asia (most probable from China) during 2014-2016 (Bastasch 2017; Montzka et al. 2018; NASA 2018a; WMO 2018a). Penetrating to the lower stratosphere, CFC-11 contributes to destroying ozone leading to a reduction of Earth protection from an increased penetration of solar ultraviolet B radiation (UV-B) to the earth surface and intensification of global warming (Ward 2016; UCS 2017; WMO 2018a). Previously, such situation of strong earth temperature increase, occurred from the mid-1970s, when CFC gases, manufactured worldwide since 1960, penetrated to the lower stratosphere, were broken by UV-B radiation, resulted in releasing chlorine, which destroyed a large amount of lower-stratospheric ozone (Ward 2016). Additional source of ozone depletion during 2015-2017 and increasing global temperature might be also eruption of Bardarbunga volcano from September 2014 through February 2015 in the central Iceland. This effusive-type volcano has spread mostly basaltic lava over the area of 85 km², which emitted ozone-depleting chlorine and bromine (Ward 2016). When these two gases reached the lower stratosphere in the second half of 2015, they provided additional contribution to destroying earth-protective ozone layer, increasing UV-B radiation reaching the earth surface, causing some warming (Solomon 1999; Ward 2016; UCS 2017).

38-year (1981-2018) global drought trends during intensive climate warming

The shown above very strong 4-year (2015-2018) doubling global mean TA (compare to 17-year stable global mean TA prior to that period, (1998-2014)) might likely to intensify severely global drought and change overall drought trends. Therefore, [Figure 4b](#) displays weekly global mean VHI-drought time series for the entire 38-year (1981-2018), which includes three periods of global temperature trends: (a) intensive global mean TA increase from 1981 through 1997, (b) stable positive TA during 1998-2014 and (c) 2015-2018 doubling TA (relative to 1981-2010 climatology) compare to trend level ([Figure 4a](#)). Unfortunately, the latest four-year period of TA data (case (c)) is too short for statistical trend analysis. Therefore, only visual interpretation of this period is presented. As was mentioned, global TA (relative to 1980-2010 climatology) during 2015-2018 increased more than 2 times compared to previous 17-year TA trend. In spite of doubling global TA, neither drought area nor intensity have increased, which has been erroneously expected. In general, VHI-estimated global-mean drought area and intensity has not changed between 2015 and 2018 and was relatively stable, covering 25-33% global area (variations are seasonal) for S-to-E, 12-16% for E-to-E and around 2.5% for E intensity ([Figure 4b](#)). In addition, the drought intensity and area during 2015-2018 remained at the level of the previous 7-year between 2008 and 2014, when global-mean TA was more than two-time smaller (0.15-0.22 °C compared to 0.44-0.56 °C during 2015-2018 ([Figure 4b](#))).

Stable VHI-drought activity (both area and intensity) during 2015-2018 is supported by global distribution of VHI-estimated drought for each 16 km² pixel ([Figure 5](#)). In 2015 ([Figure 5a](#)), drought was much more intensive (compared to 2014) in Africa (northern areas of sub-Saharan and Southern Africa), northeastern Australia, Western Europe and Mongolia, but North and South America showed some

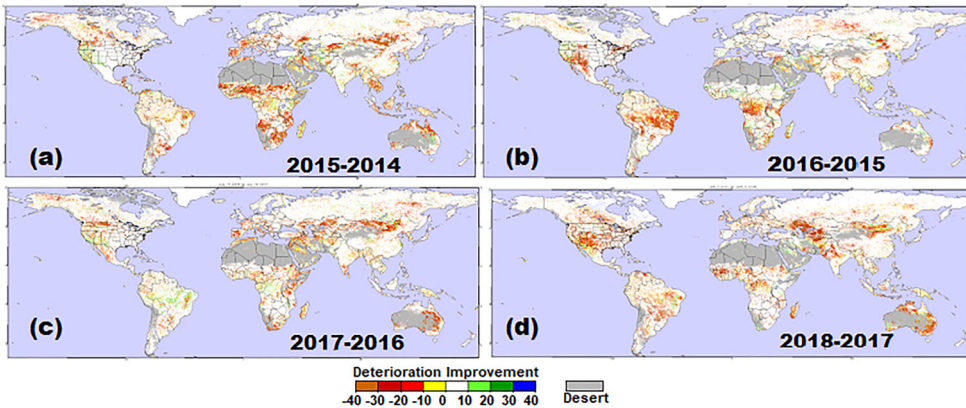


Figure 5. Area of drought deterioration or improvement (for each 16 km² pixels) between July of the two neighboring years: (a) 2015 versus 2014 (difference between VHI15 and VHI14), (b) 2016 versus 2015 (VHI16-VHI15), (c) 2017 versus 2016 (VHI17-VHI16) and (d) 2018 versus 2017 (VHI18-VHI17). Source: Author

Table 2. Rate of trend change (%) in global temperature anomaly and VHI-based global drought area/intensity from the beginning to the end of the indicated periods.

| Parameter | Period | | | |
|------------------------|-----------|-----------|-----------|-----------|
| | 1981-2018 | 1998-2018 | 1998-2014 | 1981-1997 |
| Temperature Anomaly | 284 | 200 | 20 | 183 |
| Severe-to-Exceptional | 5.5 | 5.7 | 5.3 | 10.3 |
| Extreme-to-Exceptional | -2.0 | 2.0 | 4.0 | 10.6 |
| Exceptional | 2.8 | 1.6 | 1.3 | 3.6 |

improvements (Figure 5a). Deteriorated drought area in 2015 (compared to 2014) accounted for nearly 26% of the world (excluding deserts). In 2016, drought deterioration (compared to 2015) accounted approximately similar percent of world area, but major deterioration switched to North and South America and part of central Africa (Figure 5b). From the other two cases (2017 vs 2016 and 2018 vs 2017 (Figure 5c and d)), deteriorated drought area was approximately nearly 30% of the globe but severity of drought deterioration was redistributed over the world. Summarizing this discussion, we should stress again that more than doubling global mean TA has not intensified 2015-2018 drought and has not increased its area.

Finally, we investigated if doubling global temperature anomaly during 2015-2018 (compared to 1998-2014) has changed long-term (almost four decades) global drought trends since 1981. Two drought tendencies were investigated (a) the entire period, 1981-2018 and (b) the latest 21 years (1998-2018). The two previous periods of intensive climate warming (c) 1981-1997 and hiatus time (d) 1998-2014 have been also included for comparative analysis (Table 2). Linear drought trend was statistically approximated for the time series shown in Figure 4. Parallel with drought trends, global mean TA trend was also estimated. Following these estimates, relative changes between the values of trend at the end and beginning (relative to the beginning value in %) for the investigated periods were derived, following the equation: $RD_k = 100^*$

$(t_j - t_i)/t_i$, where RD – relative difference (%), t_j – parameters' values at the trend end, t_i – values at the trend beginning.

Following Table 2, displaying these relative differences (RD), it is important to emphasize first that, when 2015-2018 extremely increased global mean TA was added to the 1981-2014 time series, the TA trend increased almost 3 times ($RD = 284\%$) during 1981-2018 and 2-time (183%) during 1998-2018. Drought area and intensity trends during the same periods have not followed 2-3 times global mean TA increase. Specifically, during the entire 38 years (1981-2018), global drought area increased negligibly, less than 5.5% (the increase was even negative (-2%) for E-to-E drought intensity). For the most recent 21-year period (1998-2018), drought area increased slightly as well (1.6-5.7%). In addition to a negligible global drought tendency, which has not followed 200-284% global mean TA increase, it is important to point out again a fairly stable 17-year temperature trend (20% increase) from 1998 through 2014 (without the latest 4-year) and very negligible (less than 5.5%) drought trend increase. The PDSI index have not shown drought area and intensity changes during 1980-2017 (BAMS 2018; Osborn et al. 2018). Summarizing this discussion, it is important to emphasize again and again that 200-300% global mean TA increase during the entire 38-year period (1981-2018) and the most recent, 21-year period (1998-2018) of global warming caused only negligible, less than 6% change in the global drought area and intensity. Regarding near-future global warming, looking at the global mean TA changes during the last 4-year: TA increase during 2015 (mean global TA 0.45°C) and 2016 (0.56°C), but TA decrease during 2017 (0.46°C) and, especially 2018 (0.33°C) returning back to previous 17-year flat trend (1998-2014). Considering climate tendency since 1980 (especially in the most recent 4-year (2015-2018)), and drought trends during strong climate warming, it is not likely to expect drought expansion and intensification.

What to expect with food security?

In the recent three-four decades, enhanced tendency in Earth population increase and gradual leveling off global grain production (the major food and feed for the world) have increased the gap between global grain supply and demand, deteriorating long-term food security (Kogan 2018). This situation has normally worsened strongly in the years of intensive droughts, when global grain supply becomes below the demand (negative balance). Unfortunately, in the first 18-year of the 21st century, eight years had a negative balance (Kogan 2018). Such years affect strongly developing countries, since the population in these countries is suffering frequently from a lack of food, leading to people's malnutrition and hunger (Kogan et al. 2019). Presented in this paper's analysis of intensive long-term Earth warming and satellite derived global drought trends have indicated that two-three times (200-284%) global mean TA increase in the latest 38-year (since 1981) has not practically changed trends in global drought area and intensity (Table 2, Figures 4 and 5). Therefore, in order to evaluate present climate warming impacts on future annual food security, the final analysis covers the most recent two-decade's (1998-2018) drought dynamics in the three major grain producing countries, China, USA and India, (producing nearly 50% of

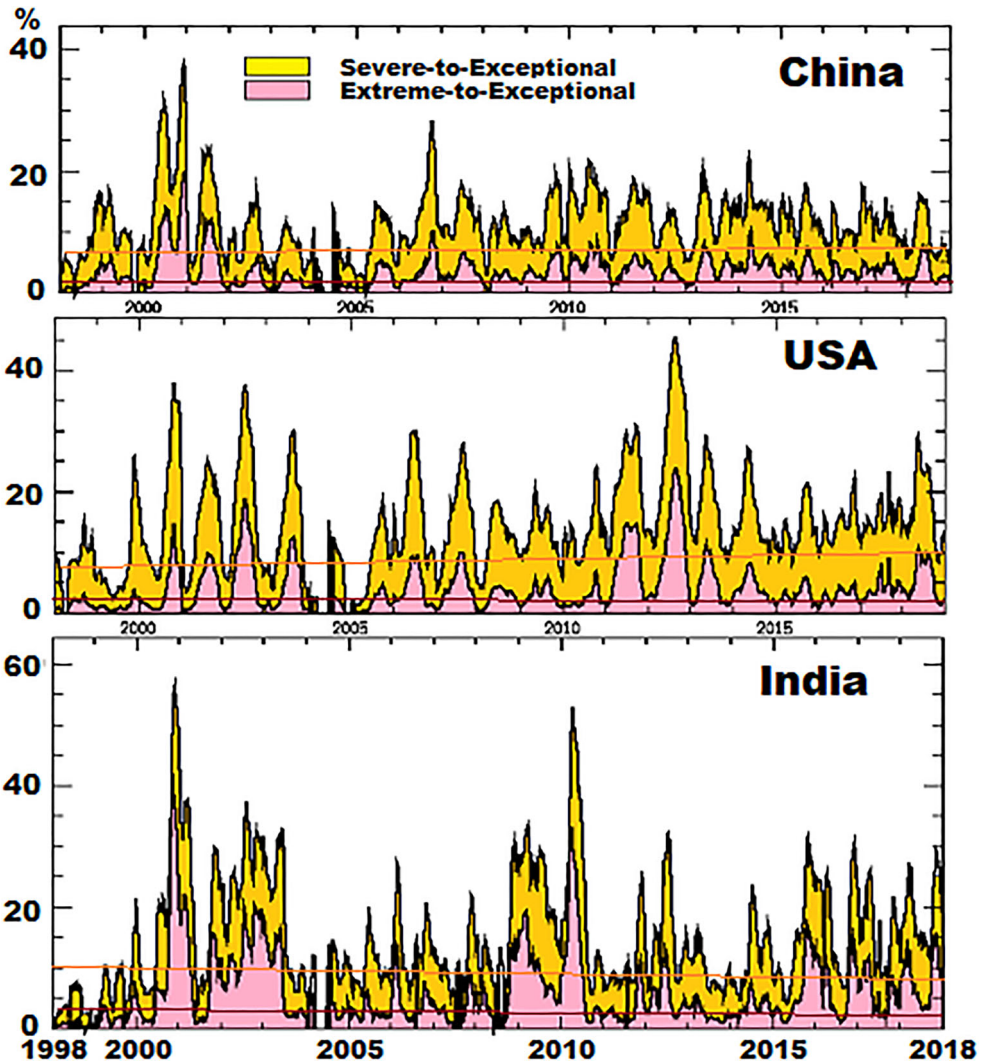


Figure 6. 1998-2018 dynamics of weekly drought area (% from country) and intensities (severe-to-exceptional (S-to-E), and extreme-to-exceptional (E-to-E) and their trends (95% confidence level) in China, USA and India. Source: Author

the world grain), since they determine much annual availability of global grain and situation with global food security.

Figure 6 shows satellite-based estimated dynamics of drought area and intensity in these three countries from 1998 through 2018. During these years, global mean TA has increased 200%, indicating strong Earth warming. However, in spite of doubling global TA during these 21-year, VHI-estimated drought trends in the major grain producing countries (Figure 6) has practically not increased, remaining at the relatively stable level for the investigated two intensities (S-to-E and E-to-E). These two intensities are specially analyzed since the grain losses are normally the largest and more frequent (Kogan 2018; Kogan et al. 2019). The 21-year general drought level for S-to-E intensity is nearly 10% in India, 7.5 and 6.2% in the USA and China,

respectively. For the stronger drought level (E-to-E) it is 2-3% for these countries. Following drought trends in Figure 6, it is noticeable a stable drought level during 21-year in China, very slight drought level increase in the USA, and very slight decrease drought level in India by 2018. Maximal drought area during the indicated 21-year, might cover up to 40% of the USA and China and up to 60% of India. In addition, China's drought more frequently covers less than 20% of country's area, while in the USA and India, 20-28% of their areas.

Conclusion

We have been living during the time of intensive global warming. Climate publications have emphasized that from the second half of 19th century, intensive Earth warming has speeded up ice melting and sea level rise, increased water shortage and drought intensity, deteriorated agricultural system and produced other changes. Experts from the United Nations are warning that continuation of climate warming, would strongly intensify and expand droughts, leading to a reduction of crop production, especially in developing countries of Africa, Asia and Latin America, further deteriorating food security and intensifying population's malnutrition and hunger in poor countries. The recent 20-year climate-change scientific publications regarding drought dynamics and impacts on the Earth living are based on less than two decades of low-resolution weather station data for a relatively local areas, rather than on analysis of multi-decadal global and the main agricultural countries' high-resolution drought records. Since climate warming is still continuing, it is important to estimate global and main agricultural regions drought trends, based on high resolution data, and predict a near future drought development and its potential impacts on food security. This can be effectively done using high-resolution (4 and 16 km²) satellite data, which are available in operational mode from 1981, exactly during the period of intensive global warming. This investigation was possible due to availability of new physiologically based satellite-derived Vegetation Health (VH) method. Following high-resolution (both special and temporal) global, 38-year vegetation health assessments, it was possible to prepare long-term satellite data and process them statistically in order to: (a) obtain global and regional drought dynamics (area and intensity), (b) determine drought trends, (c) derive if drought trend is following global temperature increase, claimed by climate publications and (d) predict what consequences should be anticipated with food security. Important that (1) satellite-derived Vegetation Health indices were comprehensively calibrated and cleared from long- and short-term noise; (2) droughts were estimated from vegetation's thermal and moisture conditions; (3) 38-year VH data were used for drought trend analysis; (4) assessments were done for the entire world and the main grain-producing countries, (5) original VH data had 1, 4 and 16 km² areal and one-week temporal resolution data, which were validated in 32 countries covering all continents.

Following the analysis of global climate records since 1981, two 17-year Earth warming periods were clearly identified: 1981-1997 with strong global mean TA increase (from -0.32 to $+0.2$ °C) and 1998-2014 with stable TA (around $+0.2$ °C) trend during the hiatus period. Global and hemispheric VH-derived two 17-year

drought trends have completely mismatched with global TA trends. Specifically, drought area and intensity (in all categories) remained stable, although the world warmed up strongly (TA increased (based in 1980-2010 climatology) more than 0.5 °C) between 1981 and 1997. However, during the hiatus time (1998-2014), when global TA was stably warm (0.2 °C), droughts have intensified and their area increased, especially in Southern Hemisphere. Moreover, in China, USA and India, the major grain-producing countries (nearly 50%), drought area for Severe-to-Exceptional intensity reduced during 1981-2014, while the Earth was warming up strongly, mismatching again with drought trend. During 2015-2018, global mean TA strongly increased following ocean heat release, especially from 2015-16 El Niño and chlorine/bromine-based ozone depletion in the lower stratosphere. However, CO₂ increase from 2014 to 2015 was too small to contribute to global temperature increase. Meanwhile, more than doubling 4-year global mean TA (compared to 1998-2014 period) has not intensified the 2015-2018 drought and has not increased its area. For the entire 38-year (1981-2018) and the latest 21-year (1998-2018), two-three times increased global Earth warming has not changed drought area and intensity. Following the presented 38-year satellite data, it is possible to state firmly that global and main grain countries' drought area and intensity trends have not been following global climate warming since 1980's. Further investigation should investigate drought trends in a few other countries, secondary-level producers of grain, such as Russia, Argentina, Australia and others.

Disclosure statement

No potential conflict of interest was reported by the authors.

ORCID

Wenze Yang  <http://orcid.org/0000-0001-8514-2742>

References

- BAMS. 2018. NOAA: state of the climate highlights 2018. Bulletin of the American Meteorological Society. 99(8), 18–46. <https://snowbrains.com/noaa-bams-state-climate-2017/>.
- Bastasch M. 2017 Jun 2. China is “Sticking to the Paris agreement in name only, its plans show a much different intent”. *The Daily Signal*. <https://www.dailysignal.com/2017/06/02/china-is-sticking-to-the-paris-agreement-in-name-only-its-plans-show-a-much-different-intent/>. Accessed Feb 2018.
- Blander J, Arndt DS, and Hartfield G, editors. 2018. State of the climate in 2017. Bull Am Meteor Soc. 99(8):Si–S310.
- Bromwich DH, Nicolas JP, Monaghan AJ, Lazzara MA, Keller LM, Weidner GA, Wilson AB. 2013. Central West Antarctica among the most rapidly warming regions on earth. *Nature Geosci*. 6(2):139–145.
- Brown LR. 2012. Full planet, empty plates: the new geopolitics the food scarcity. Earth Policy Institute; p. 79; www.earth-policy.org. Accessed Jul 2017
- Brown LR. 2013 Feb 6. Global grain stocks drop dangerously low as 2012 consumption exceeded production. Sustainable Agriculture. <https://books.google.com/books?id=gft1CQAAQBAJ&pg=PT262&lpg=PT262&dq=Brown+LR.+2013+Feb+6&source=bl&ots=Vd>

Qucwws6P&sig=ACfU3U3IfeZzvOke9uyx0v7HqM_uDzg3jg&hl=en&sa=X&ved=2ahUKEwjVlJT3r9TnAhWKhXIEHSjkAEcQ6AEwAXoECAUQAQ#v=onepage&q=Brown%20LR.%202013%20Feb%206&f=false

- Charles H, Godfray J, Beddington JR, Crute R, Haddad L, Lawrence D, Muir JF, Pretty J, Robinson S, Thomas SM, et al. 2018. Food security: the challenge of feeding 9 billion people. *Food Security*. https://waterlandandecosystems.wikispaces.com/file/view/Component2_CIAT.pdf. Accessed Dec 2018.
- Chandler DL. 2018 Feb 13. MIT News. <http://news.mit.edu/2018/intensive-agriculture-influences-us-regional-summer-climate-0213>. Accessed Dec 2018.
- Cheng L, Abraham J, Hausfather Z, Trenberth KE. 2019. How fast are the ocean warming? *Science*. 363(6423):128–129.
- Christy JR. 2017 Mar 29. Testimony to U.S. House Committee on Science, Space & Technology. <https://science.house.gov/sites/republicans.science.house.gov/files/documents/HHRG-115-SY-WState-JChristy-20170329.pdf>. Accessed Dec 2018.
- Coats DR. 2018 Feb 13. Worldwide threat assessment of the US Intelligence Community. p. 25. https://www.wilsoncenter.org/article/world-wide-threat-assessment?gclid=EAIaIQobChMI8uL_89nZ4AIVFlmGCh2YGgXoEAAAYASAAEgI1GfD_BwE. Accessed Jan 2019.
- Cornwall W. 2019. In hot water. *Science*. 303(6426):442–445.
- Eilpering J, Dawsey J, Dennis B. 2019 Feb 26. Panel to fight climate science. *Washington Post (Express)*. p. 11.
- FAO. 2017. How close we are to zero hunger. <http://www.fao.org/state-of-food-security-nutrition/en/>. Accessed Mar 2018.
- FAO. 2018. FAO cereal supply and demand brief. *World Food Situation*. <http://www.fao.org/worldfoodsituation/csdb/en/>. Accessed Dec 2019.
- Forzieri G, Alkama R, Miralles DG, Cescatti A. 2017. Satellites reveal contrasting responses of regional climate to the widespread greening of Earth. *Science*. 356(6343):1180–1184.
- Godfray HCJ, Beddington JR, Crute IR, Haddad L, Lawrence D, Muir JF, Pretty J, Robinson S, Thomas SM. 2010. Food Security: The Challenge of Feeding 9 Billion People. *Science*, 327, 812–818. <http://dx.doi.org/10.1126/science.1185383>
- Hansen J, Sato M, Ruedy R, Lacis A, Oinas V. 2000. Global warming in the twenty-first century: an alternative scenario. *Proc Natl Acad Sci USA*. 97(18):9875–9880.
- Hansen JE, Ruedy R, Sato M, Lo K. 2010. Global surface temperature change. *Rev Geophys*. 48(4):RG4004.
- Hartfield G, Blunden J, Arndt DS. 2018. A look at 2017. *Bull Am Meteor Soc*. 99(8): 1527–1539.
- Hashemi SA, Chenani SK. 2004. Investigation of NDVI index in relation to chlorophyll content change and phenological events. *Recent Advances in Environment, Energy Systems and Naval Science*. <http://www.wseas.us/e-library/conferences/2011/Barcelona/MNICEG/MNICEG-02.pdf>. Accessed Jun 2016.
- IPCC. 2007. Climate change 2007: synthesis report. Geneva, Switzerland. p. 104. https://www.ipcc.ch/publications_and_data/publications_ipcc_fourth_assessment_report_synthesis_report.htm. Accessed 2008.
- IPCC. 2014. Climate change 2014, *Synthesis report*. 5th assessment (Pachauri, RK, Meyer L, editors.). Geneva, Switzerland, p. 151. https://www.ipcc.ch/pdf/assessment-report/ar5/syr/SYR_AR5_FINAL_full_wcover.pdf. Accessed 2015
- IPCC. 2018a. Climate change 2014 Synthesis report summary for policymakers. https://www.ipcc.ch/site/assets/uploads/2018/02/AR5_SYR_FINAL_SPM.pdf. Accessed 2019.
- IPCC. 2018b. Global warming 1.5 °C: summary for policy makers. https://www.ipcc.ch/site/assets/uploads/sites/2/2018/07/SR15_SPM_High_Res.pdf. Accessed Dec 2018.
- Karl TR, Arguez A, Huang B, Lawrimore JH, McMahon JR, Menne MJ, Peterson TC, Vose RS, Zhang H-M. 2015. Possible artifacts of data biases in the recent global surface warming hiatus. *Science*. 348(6242):1469–1472.
- Kennel CF. 2014. Hiatus in global warming. Scripps Institute of Oceanography. <https://olli.ucsd.edu/display/documents/ClimateChange.pdf>. Accessed Dec 2014.

- Kogan F. 2018. Remote sensing for food security. Switzerland, Springer; p. 255.
- Kogan F, Adamenko T, Guo W. 2013. Global and regional drought dynamics in the climate warming era. *Remote Sens Lett.* 4(4):364–372.
- Kogan F, Goldberg M, Schott T, Guo W. 2015. SUOMI NPP/VIIRS: improve drought watch, crop losses prediction and food security. *Int J Remote Sens.* 36 (21), 1–11.
- Kogan F, Guo W. 2014. Early twenty-first-century droughts during the warmest climate. *Geomatics Nat Hazards Risk.* 1–7:1 127–137
- Kogan F, Guo W. 2017. Strong 2015–2016 El Niño and implications to global ecosystems from space. *Int J Rem Sens.* 38(1):161–178.
- Kogan F, Guo W, Yang W. 2019. Drought and food security prediction from NOAA new generation of operational satellites. *Geomatics Nat Hazards Risk.* 10(1):651–664.
- Kogan F, Guo W, Yang W, Shannon H. 2018. Space-based vegetation health for wheat yield modeling and prediction in Australia. *J. Appl. Remote Sens.* 12(2):026002.
- Kogan FN. 1983. Perspectives for grain production in the USSR. *J. Agric Meteorol.* 28(3): 213–227.
- Kogan FN. 1997. Global drought watch from space. *Bull Am Meteor Soc.* 78(4):621–636.
- Kogan FN. 2001. Operational space technology for global vegetation assessment. *Bull Am Meteor Soc.* 82(9):1949–1964.
- Lucht W, Prentice IC, Myneni RB, Sitch S, Friedlingstein P, Cramer W, Bousquet P, Buermann W, Smith B. 2002. Climate control of the high-latitude vegetation greening trend and Pinatubo effect. *Science.* 296(5573):1687–1688.
- Montzka SA, Dutton GS, Yu P, Ray E, Portmann RW, Daniel JS, Kuijpers L, Hall BD, Mondeel D, Siso C, et al. 2018. An unexpected and persistent increase in global emission of ozone-depleting CFC-11. *Nature.* 557(7705):413–417.
- Murph BF, Timbal B. 2008. A review of recent climate variability and climate change in southeastern Australia. *Int J Climatol.* 28:859–879.
- Myneni RB, Keeling CD, Tucker CJ, Asrar G, Nemani RR. 1997. Increased plant growth in the northern high latitudes from 1981–1991. *Nature.* 386(6626):698–702.
- Najafi E, Devineni N, Khanbilvardi RM, Kogan F. 2018. Understanding the changes in global crop yields through changes in climate and technology. *Earth's Fut.* 6(3):410–427.
- NASA. 2017. Global climate change: global land-ocean temperature. <https://climate.nasa.gov/vital-signs/global-temperature/>. Accessed Jul 2018.
- NASA. 2018a. Ozone Watch. <https://ozonewatch.gsfc.nasa.gov/>. Accessed Dec 2018.
- NASA. 2018b. Global climate change. <https://climate.nasa.gov/vital-signs/carbon-dioxide/>. Accessed Feb 2019.
- Nemani RR, Keeling CD, Hashimoto H, Jolly WM, Piper SC, Tucker CJ, Myneni RB, Running SW. 2003. Climate-driven increases in global terrestrial net primary production from 1982 to 1999. *Science.* 300(5625):1560–1563.
- NOAA. 2016. Global climate report. www.ncdc.noaa.gov/cag/time-series/global. Accessed Sep 2017
- NOAA. 2017. Global climate report – November. December. <https://www.ncdc.noaa.gov/sotc/global/201711>.
- NOAA/NCEI. 2017 Apr. State of the climate: global climate report for March 2017. <https://www.ncdc.noaa.gov/sotc/global/201703>. Accessed Dec 2017
- NOAA/NESDIS. 2019. Vegetation Health indices and products. <https://www.star.nesdis.noaa.gov/smcd/emb/vci/VH/index.php>. Accessed Nov 2019.
- Osborn TJ, Barichivich J, Harris I, van der Shrier G, Jones PD. 2018. Drought. *Bull Am Met Soc.* 99(8):536–539. <https://snowbrains.com/noaa-bams-state-climate-2017/>.
- Seager R. 2018. Whither the 100th meridian? The once and future physical and human geography of America's arid–humid divide. Part I: the story so far. *Earth Interact.* 22(5):1–22.
- Serreze MC. 2018. *Brave New Arctic the untold story of melting north.* Princeton University Press; p. 269. Princeton, USA.
- Solomon S. 1999. Stratospheric ozone depletion: a review of concepts and history. *Rev Geophys.* 37(3):275–316.

- Spencer RW. 2019 Jan 30. *The 2018 global mean surface temperature anomaly (climatology 1981–2010)*. <http://www.drroyspencer.com/2019/01/uah-global-temperature-update-for-december-2018-0-25-deg-c/>. Accessed Feb 2019.
- Thomas L, Frölicher TL, Fischer EM, Gruber N. 2018. Marine heatwaves under global warming. *Nature*. 560:360–364.
- Toulmin C. 2010. Food security: the challenge of feeding 9 billion people. *Science*. 327:812–818.
- Trishchenko AP. 2006. Solar irradiance and effective brightness temperature for SWIR channels of AVHRR/NOAA and GOES imagers. *J Atmos Ocean Technol*. 23(2):198–210.
- Tucker CJ. 1979. Red and photographic infrared linear combination for monitoring vegetation. *Rem Sens Environ*. 8(2):127–150.
- [UCS] Union of Concerned Scientist. 2017 Jul 17. Is there a connection between the ozone hole and climate warming? <https://www.ucsUS.org/global-warming/science-and-impacts/science/ozone-hole-and-gw-faq.html#.Wrgcs4jwaUl>. Accessed Dec 2018.
- UNESCO. 2018. Climate change and water security. <https://en.unesco.org/themes/addressing-climate-change/climate-change-and-water-security> Accessed Jan 2019.
- USGCRP. 2017. In: Wuebbles DJ, Fahey DW, Hibard KA, Dokken DJ, Steward BC, Maycock TK, editors. *Climate science special report: fourth national climate assessment*. Vol. 1. Washington (DC): US Global Change Research Program; p. 470.
- Ward PL. 2016. *What really causes global warming?* New York (NY): M & J Publishing Co; p. 235.
- Watts J. 2018 Mar 19. Water shortages could affect 5bn people by 2050, UN report warns. *The Guardian*. <https://www.theguardian.com/environment/2018/mar/19/water-shortages-could-affect-5bn-people-by-2050-un-report-warns>. Accessed Jan 2019.
- WB. 2017. Agriculture & rural development. <https://data.worldbank.org/topic/agriculture-and-rural-development>. Accessed Oct 2019.
- Wendel J. 2018. Global average temperature in 2017 continue upward trend. *EOS Earth Space Sci News*. 99(3):3–4.
- Williams RG, Roussenov V. 2017. Sensitivity of global warming to carbon emissions: effects of heat and carbon uptake in a suite of earth system models. *J Clim*. 30(23):9343–9363.
- WMO. 2014. Global surface temperature data sets. http://www.wmo.int/pages/prog/wcp/wcdmp/GCDS_3.php. Accessed Apr 2016.
- WMO. 2016 Jan 25. 2015 is the hottest year on record. <https://public.wmo.int/en/media/press-release/2015-hottest-year-record>. Accessed Apr 2018
- WMO. 2017. WMO statement on the state of climate in 2017. WMO#1220. https://library.wmo.int/doc_num.php?explnum_id=4453. Accessed Apr 2018.
- WMO. 2018a. Executive summary: scientific assessment of ozone depletion. World Meteorological Organization, Global Ozone Research and Monitoring Project – Report #5. Geneva (Switzerland); p. 67.
- WMO. 2018b Nov 29. WMO climate statement: past 4 years warmest on record. <https://public.wmo.int/en/media/press-release/wmo-climate-statement-past-4-years-warmest-record=898> Accessed Dec 2018.